XVI IMEKO World Congress
Measurement - Supports Science - Improves Technology - Protects Environment ... and Provides Employment - Now and in the Future
Vienna, AUSTRIA, 2000, September 25-28

ACCURACY OF HARMONIC ANALYSIS OF CIRCULAR PROFILES

S. Zebrowska-Lucyk
Institute of Metrology and Measuring Systems
Warsaw University of Technology, Warsaw, Poland

Abstract: The paper deals with the Fourier spectrum of nominally round profiles measured by the radius method [1]. It is shown that amplitudes and phases of individual harmonics found by this method depend on the distance between the geometric centre of the investigated cross-section of the specimen under measurement and the centre of rotation as well as of the position of the sensor. On the grounds of a theoretical analysis, mathematical relations that describe the phenomenon of modulation of profile's harmonics has been worked out. The paper describes conditions under which the eccentricity of a nominally round profile in relation to the centre of rotation causes complete attenuation of individual harmonics. Numerical simulations and experiments performed by means of computerised roundness measuring systems entirely confirmed theoretical analysis.

Keywords: harmonic analysis, roundness, Fourier series, eccentricity

1 INTRODUCTION

In mechanical engineering industry recognition of harmonic components of nominally round profiles is usually accomplished on the basis of measurements by the radius method [1, 2]. Most of the newest instruments that perform roundness measurements by this method are equipped with software, which enables the user to separate individual frequencies and to find predominant numbers of undulations per revolution [3, 4].

While applying analogue or numerical wave filters give the effect on non-roundness of several undulations within a relatively broad frequency band, harmonic analysis lets the user to focus on a single harmonic. Detection of harmonics that have predominant amplitudes allows, on the one hand, to identify the shape deviation sources inherent in a manufacturing process, and on the other hand, to foresee some exploitation properties of investigated elements. Especially the latter application requires high accuracy calculations of the individual harmonics. Both numbers and amplitudes of dominant harmonics should be precisely identified. For instance, the properties of a bearing roll that have 11 undulations on circumference are completely different from properties of a roll with 12 undulations of the same amplitude.

The paper shows that in some cases the eccentricity of an investigated profile in relation to the axis of rotation as well as inaccurate position of the sensor in relation to this axis causes significant deformations of the profile spectrum. To examine the effects of distortion of individual harmonics three methods have been applied: analytical, numerical simulation and experiments.

2 RELATIONSHIP BETWEEN PROFILE AND OUTPUT SIGNAL

Figure 1 shows the most general case of measurement of a nominally round profile by the radius method. The sensor rotates around point 0_2. The point 0_1 is centre of the investigated profile's mean circle The distance between points 0_1 and 0_2 equals e. The line of movement of the sensor's tip centre misses the centre of rotation 0_2 by the distance l.

Projection AS of the instantaneous distance from the tip centre to the centre of rotation on the direction of movement of the sensor tip (SO_2) is denoted by symbol r_p. It can be expressed by the following Equation:

$$r_p(j_p) = e\cos(j_p - q) + \sqrt{r_z^2 - \left(l + e\sin(j_p - q)\right)^2} \qquad (1)$$

where:

- j_p - angle between the instantaneous measuring direction and axis of the polar system
- r_z - distance between the investigated profile's centre and the tip's centre (O_1S), further on called the substitute radius

The substitute radius equals:

in external surfaces measurements : $r_z = r_{el} + r_k$ (2a)
in internal surfaces measurements: $r_z = r_{el} - r_k$ (2b)

where:

r_{el} - radius of the investigated profile (O_1C) in the point of contact with the sensor's tip
r_k - sensor tip's radius (CS).

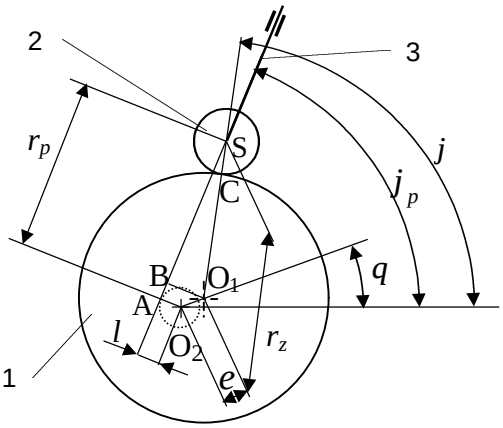

Figure 1. Measurement of roundness; e - eccentricity (O_1, O_2), l - distance of the displacement line of the tip centre from the centre of rotation O_2 (AO_2), r_z - substitute radius (SO_1), r_p - apparent radius (SA.); 1 - profile under measurement, 2 - sensor tip, 3 - sensor arm

Projection AS of the instantaneous distance from the tip centre to the centre of rotation on the direction of movement of the sensor tip (SO_2) is denoted by symbol r_p. It can be expressed by the following Equation:

$$r_p(j_p) = e\cos(j_p - q) + \sqrt{r_z^2 - \left(l + e\sin(j_p - q)\right)^2} \quad (1)$$

where:

j_p - angle between the instantaneous measuring direction and axis of the polar system
r_z - distance between the investigated profile's centre and the tip's centre (O_1S), further on called the substitute radius

The substitute radius equals:

in external surfaces measurements : $r_z = r_{el} + r_k$ (2a)
in internal surfaces measurements: $r_z = r_{el} - r_k$ (2b)

where:

r_{el} - radius of the investigated profile (O_1C) in the point of contact with the sensor's tip
r_k - sensor tip's radius (CS).

The instantaneous substitute radius r_z can be expressed by the sum of two components:

$$r_z(j) = r_{zo} + \Delta r_z(j) \quad (3)$$

where:

r_{zo} – radius of the mean circle of the profile,
φ – instantaneous angle with the corner in the point O_1,
$\Delta r_z(j)$ – instantaneous deviation of the investigated profile from the mean circle.

Let r_{po} stand for the radius-vector of a perfectly round profile, i.e., $\Delta r_z(j) = 0$. It is written as follows:

$$r_z = r_{zo} = const \qquad r_p(r_{zo}, j_p) = r_{po}(j_p) \quad (4a, 4b)$$

Since $\Delta r_z(j)$ is always very small in comparison with r_{zo}, it is possible to write

$$r_p\left(r_z(j), j_p\right) = r_{po}(j_p) + \Delta r_p(j_p) \quad (5)$$

where

$$\Delta r_p(j_p) = \left.\frac{\partial r_p}{\partial r_z}\right|_{r_z = r_{zo}} \Delta r_z(j_p) \quad (6)$$

The derivative that occurs in Eq. (6) can be approximated by the following Equation resulting from (1):

$$\left.\frac{\partial r_p}{\partial r_z}\right|_{r_z = r_{zo}} \cong 1 + \frac{1}{r_{zo}^2}\left(\frac{2l^2 + e^2}{4} + el\sin(j_p - q) - \frac{e^2}{4}\cos 2(j_p - q)\right) \quad (7)$$

Fourier spectrum of the sensor output signal $r_p(\varphi_p)$ can be found by separate calculations of the spectrum of each from the right–hand side components of Eq. (5).

Spectrum of the first component (r_{po}), which corresponds to measurements of a perfectly round profile when e and l are not equal to zero has been found by author and described in [5]. In this paper only most important results are quoted (Section 3).

It would be very complicated to find the output spectrum for any arbitrary profile's irregularities. Therefore considerations were delimited to the case when the radius increase $\Delta r_z(\varphi)$ is expressed by a single harmonic or a few harmonics distinctly different as regards frequencies (see Section 4). Selection of such a model is justified since in practice researchers and users focus their attention on harmonics that have amplitudes significantly higher than the adjoining ones.

3 FOURIER SPECTRUM OF PERFECTLY ROUND PROFILES

In this particular case, when the radius of profile is constant and equals r_{zo}, the measuring signal (output signal) analysed within the period $0 \le \varphi < 2\pi$ can be according to [5] described by the following Equation:

$$r_{po}(j_p) - g \cong (c_{po} - g) + \sum_{n=1}^{3} c_{pn} \cos(n j_p - y_{pn}) \tag{8}$$

where:

c_{pn} - amplitude of measuring signal n-th harmonic,

y_{pn} - initial phase of n-th harmonic,

g - a reference value, which is usually not precisely known.

Harmonics higher than of 3th order are so low that in practice they do not matter. Equations for estimation of first three amplitudes and phases are given in Table 1. They are not in full agreement with popular views. In common opinion the amplitude of the first harmonic is equal to the profile eccentricity e and mean value of the measuring signal is independent of the eccentricity. It is also supposed that an observed increase of the mean value of the signal is equal to an adequate increase of the profile's mean radius. However, the above Equations show it is true only for a case when the element and the sensor are very carefully positioned in relation to the axis of rotation (i.e., when e/r_{zo} and l/r_{zo} equals zero).

Table 1. Harmonics of perfectly round but eccentric profiles

N^o	AMPLITUDE	PHASE	
0	$c_{po} = (r_z - g) - \frac{l^2}{2r_z} - \frac{e^2}{4r_z}$		(8a)
1	$c_{p1} = e\sqrt{1 + \frac{l^2}{r_z^2}}$	$y_{p1} = q - \frac{l}{r_z}$	(8b, c)
2	$c_{p2} = \frac{e^2}{4r_z}$	$y_{p2} = 2q$	(8d, e)
3	$c_{p3} = \frac{e^3 l}{8r_z^3}$	$y_{p3} = 3q + 0.5p$	(8f, g)

It results from Eq, (8a) that when the sensor is fixed in a constant distance from the axis of rotation (l = const, g = const), the mean value of the signal c_{p0} varies with the change of profile eccentricity e. An increase of e causes a decrease of measuring signal mean value. The decrease is nearly proportional to e^2. Eq. (8b) reveals that if a cross-section remains in the same distance from the axis of rotation (e = const), an increase of the absolute value of l causes - apart of an obvious decrease of the signal mean value (8a) - also an increase of the first harmonic's amplitude. That increase is nearly proportional to l^2. Additionally, a linear shift of initial phase of first harmonic occurs (8c). Eq. (8d) prove that perfectly round but eccentric profiles provide also a second harmonic with the amplitude c_{p2} proportional to e^2.

The influence of e and l parameters on amplitudes of individual harmonics is inversely proportional to the substitute radius r_z.

4 FOURIER SPECTRUM OF PROFILES WITH REGULAR UNDULATIONS

Let us analyse the measurements of a profile that has n regular undulations with amplitude c_n and initial phase j_{on}:

$$\Delta r_z(j) = c_n \cos(n j - j_{on}) \tag{9}$$

Taking into consideration the relationship between j and j_p, it was obtained:

$$\Delta r_z(j_p) \cong c_n \cos\left[n\left(j_p + \frac{l + e\sin(j_p - q)}{r_{zo}} \right) - j_{on} \right] \tag{10}$$

After substituting (7) and (10) to (6) and transforming:

$$\Delta r_p(j_p) \cong c_n q_o \cos(n j_p + x \sin(j_p - q) + g) \tag{11}$$

where:

$$q_o = 1 + \frac{2l^2 + e^2}{4 r_{zo}^2} \qquad x = n\frac{e}{r_{zo}} \qquad g = n\frac{l}{r_{zo}} - j_{on} \tag{12a, b, c}$$

From formulae (11) and (12) it follows that – due to the profile's eccentricity – a single sinusoidal wave (9) transforms itself into a phase–modulated wave.
Eq. (11) can be transformed into

$$\Delta r_p = c_n q_o \left\{ J_0(x)\cos(n j_p + g) + \sum_{v=1}^{\infty} J_v(x)\left[\cos((n+v) j_p + g - vq) + (-1)^n \cos((n-v) j_p + g + vq) \right] \right\} \tag{13}$$

where $J_v(x)$ – Bessel function of the first kind and v-th order.

Eq. (13) shows that n-th order harmonic on a nominally round profile reveals in the output signal as the sum of the n-th harmonic and the infinite number of harmonics with the amplitudes pair-symmetric to the order n.

Ratio of amplitudes of harmonics in the modulated output spectrum c'_{n+v} to the original amplitude c_n, further on called the transmission coefficient $k_{n;n}$, equals:

$$k_{n;n}(x) = \frac{c'_{n+n}(x)}{c_n} = q_o J_n(x) \cong J_n(x) \tag{14}$$

Approximation in Eq. (14) is made as the coefficient q_o equals nearly 1 – see Eq. (12a).

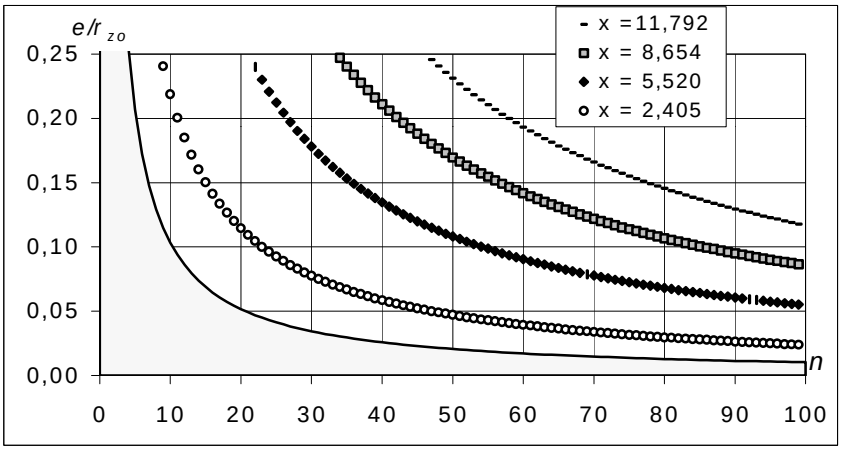

Figure 2. Particular values of the measured profile relative eccentricity; dotted lines correspond to disappearance of the n-th order original harmonic ($k_{n;0} = 0$); full line illustrates $k_{n;0} = 0{,}75$

From the shape of the Bessel curves it follows that an increase of x (i.e. increase of n for constant e and r_{zo}), flattens and widens the spectrum. For high n numbers, many spectral lines neighbouring to the line representing the original wave can appear. Eq. (14) allows predicting such particular cases when an original harmonic does not come into view at all in the output signal. These cases correspond with $J_o(x) = 0$, i.e., with following x values: $x_1 = 2{,}405$; $x_2 = 5{,}520$; $x_3 = 8{,}654$; $x_4 = 11{,}792$. Such cases are shown in Figure 2. Four dotted lines show relative eccentricities e/r_{zo}, for which the transmission coefficient $k_{n;0}$ defined by Eq. (14) equals zero. For example, the 40 harmonic fades away from the

output signal ($k_{40;0} = 0$) for three values of eccentricity, when e/r_{zo} equals 0.060, 0.138 and 0.216. On the basis of (14) It is also possible to specify such combinations of n and e/r_{zo} for which original harmonics are attenuated only to a small degree. In Fig (2) the full line corresponds to transmission coefficient $k_{n;0} = 0.75$ and the area below represents $0.75 \le k_{n;0} \le 1$. For instance, $k_{40;0} = 0.75$ when $e/r_{zo} = 0.026$.

5 DISCUSSION OF EXPERIMENTS

In order to verify results of theoretical considerations numerical simulations and practical investigations (measurements) were performed. Simulations fully confirmed the theory and yet they had to be omitted in this paper due to narrow space.

Agreement between analytical and numerical methods, although speaks in favour of the correctness of both of them, does not constitute the unquestionable proof, since the two method base on the same, strictly geometrical model.

For measurements, such elements were chosen which had cross-section profiles with nearly regular undulations. Their amplitude spectrum contained at least one harmonic predominant in the midst of other ones. The element was being placed in various random positions with respect to the axis of rotation; chosen profile was repeatedly measured and its spectrum was calculated. During analysing of obtained results, special attention was given to the effect of the eccentricity e on the amplitude of dominant harmonic C_d

Exemplary results of examination of a roller with the diameter of 12 mm by a probe with tip's radius of 1.25 mm are shown in Figure 3. Graph 3a illustrates shape deviations of the investigated profile in the polar coordinates. The graph was obtained after rather precise centring of the measured cross-section (e = 20 µm). It reveals a few dozen regular sinusoidal undulations. The angular period of undulations amounts to about 6^o.

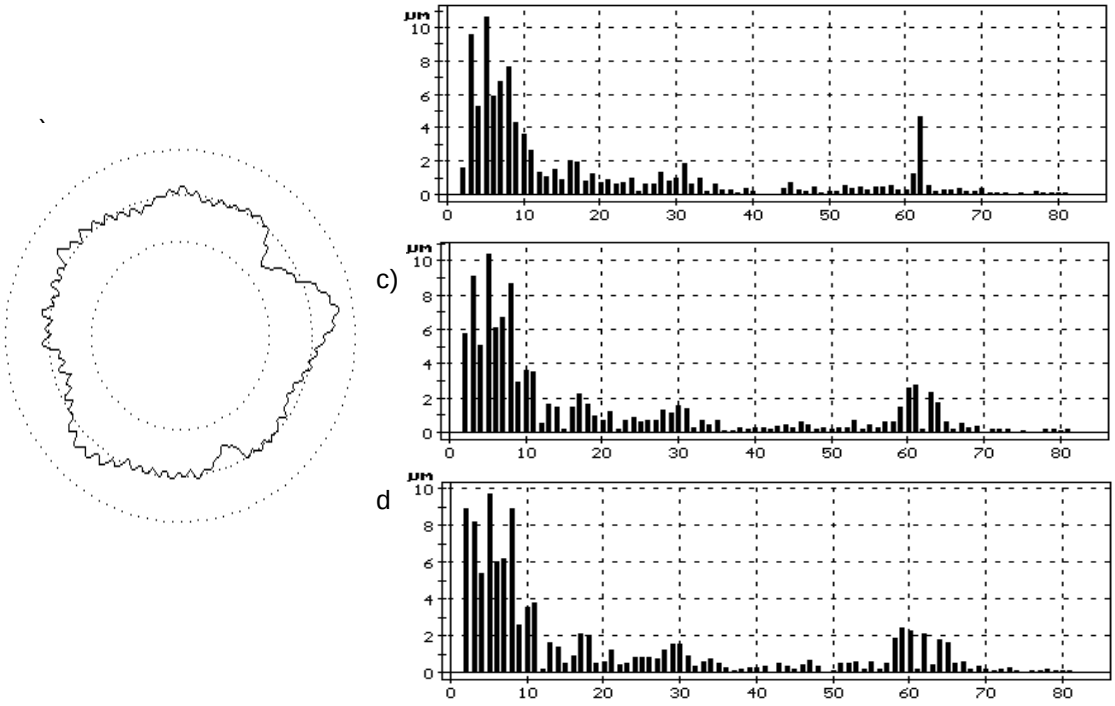

Figure 3. Measurement results of a cross-section profile: a) polar graph of roundness deviations, b) amplitude spectrum while precise positioning (e = 20 µm), c) spectrum for e = 290 µm, d) spectrum for e = 460 µm

The profile's harmonic spectrum calculated from 512 profile points is presented in diagram 3b. The 62-nd harmonic is considerably higher than its neighbours are. Its amplitude equals $C_d = C_{62} = 4.62$ µm. Next diagrams (3c and 3d) demonstrate how the spectrum changes for increasing values of e. The spectrum corresponding to e = 290 µm is shown in Figure 3c. The column that denotes 62-nd harmonic is barely visible for very low amplitude. It amounts to $C_{62} = 0.16$ µm. When e further increases, the amplitude of this harmonic increases again. For instance, $C_{62} = 2.1$ µm corresponds to e = 460 µm (Figure 3d).

More of C_{62} values obtained empirically for various eccentricities of the same element are shown in Figure 4. It is easy to remark that points of the diagram range along a curve similar for the shape to absolute values of the Bessel function of the first kind, zero order. Minimum of data corresponds to e = 290 µm (compare Fig. 3c). In theory, according to (12b) i (14), the first fading of the individual harmonics falls on:

$$e = \frac{2.405}{n} r_{zo} \tag{15}$$

For n = 62 and r_{zo} = 7.25 mm (as r_{el} = 6 mm, r_k = 1.25 mm) result of calculations is e = 281 µm.

The curve that was analytically calculated for this case and drawn in the same system of co-ordinates as data from experiment fully confirmed correctness of theoretical considerations (Figure 4).

Measurement results obtained for other investigated elements yielded similar observations

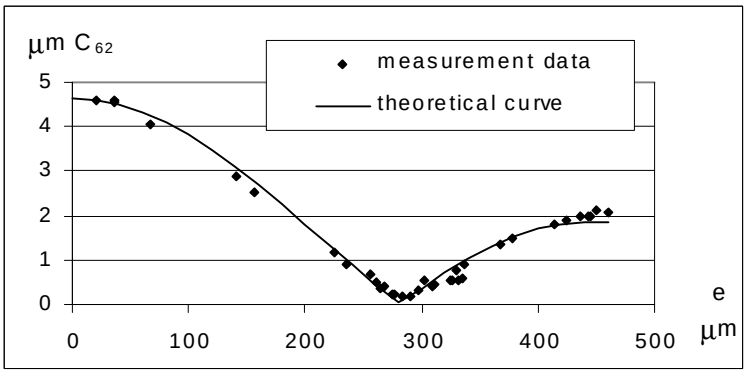

Figure 4. 62-nd order harmonic amplitude of an investigated profile vs the profile eccentricity; r_{zo} = 7,25 mm

6 FINAL REMARKS

Results of Fourier analysis in roundness measurement by the radius method are subject to positioning errors. Theoretical and empirical investigations revealed that in particular cases some harmonics might completely disappear from the input signal even if they have very high amplitudes on the examined profile. The effect of spectrum modulation is especially severe while measuring small diameter holes [5] as the parameter r_{zo} has a low value in this case.

The most effective way to prevent the phenomena described above is undoubtedly the very careful positioning. However, such a way is not fully satisfactory since it entails lowering of measurement effectiveness or significant increase of costs (due to necessary automation of measuring system) [6, 7]. Therefore, to solve this problem, more sophisticated numerical methods should be applied.

REFERENCES

[1] *ISO 4291* Methods for the assessment of departure from roundness - Measurement of variations in radius.
[2] S. Zebrowska-Lucyk, Measuring systems for quick detection of form deviations of the rotating workpieces type, in *Proceedings of the 6th International DAAAM Symposium "Intelligent Manufacturing Systems*" TU of Krakow, Poland, 1995, p. 371-372
[3] R. Rudzinski, W. Dabrowski, S. Zebrowska-Lucyk, System and Software Improvements for Precision Metrology Equipment used to Measure Roundness Deviation, *PAK* 2/1995, p. 30 -33
[4] Zebrowska-Lucyk S.: Computer-based compensation of positioning errors in roundness measurements of small precise holes. *Elektrotechnik und Informationstechnik*, 4/1998, pp. 192-197
[5] Zebrowska-Lucyk S.: The concept of an intelligent measuring and diagnostic system for analysis of form deviations, in *Proceedings of the 4th International Symposium on Measurement Technology and Intelligent Instruments*, Miskolc-Lillafüred, Hungary, 1998, p. 273-278
[6] Dutschke W., Graef J.: Zentrieren und Nievellieren auf einem Rundheitsmeßgerät. *Microtechnic*, 3 (1993), 17-19
[7] R. Bartelt, Meßunsicherheit - Ursache: Mensch *Qualitätstechniken,* 1994/39, p.1136-1141.

AUTHOR: S. ZEBROWSKA-LUCYK, Institute of Metrology and Measuring Systems, Warsaw University of Technology, ul. Chodkiewicza 8, 02-525 Warszawa, Phone Int. +048 22 6608323, Fax Int. +048 22 8490395, E-mail szl@mech.pw.edu.pl